Intelligent Management Control for Unmanned Aircraft Navigation and Formation Keeping

M. Innocenti, F. Giulietti and L. Pollini
Department of Electrical Systems and Automation
University of Pisa, Via Diotisalvi 2, 56126 Pisa, Italy

Summary

The paper presents some aspects that have become critical in the context of guidance, navigation, and control of unmanned aerial vehicles. The envisioned cost-effectiveness of unmanned air vehicles in support of a variety of military and civilian applications has introduced basic and applied research challenges in areas such as levels of autonomy and "intelligence" of the platform, interaction with manned control centers, reliability and safety of operations, and control management of single vehicle, as well as formation flights. The paper addresses issues such as dynamic modeling, formation management and control, and guidance aspects. Their origin and potential solutions are presented with particular attention to flexible formation keeping.

Issues on UAV Guidance, Navigation, Control, and Formation Flight

As of today, unmanned aerial vehicles (UAV) are being proven as cost-effective platforms for supporting military operations. Indeed, as the operational roles of such vehicles expand beyond reconnaissance, intelligence, and data gathering, to electronic warfare, ground strike, and possibly air combat, many forecast that in the near future most combat aircraft will be unmanned. Remotely controlled, semi autonomous and autonomous vehicles will also play a key role in providing services for the civilian community. UAV's can provide efficient platforms for surveillance, search and rescue, relief in natural disaster areas, and law enforcement operations. However, as the operational capabilities of unmanned vehicles develop, there is a real need for an increase in their level of autonomy, decisional capabilities among different tasks, reliable control of multi-vehicle operations, and in fight and ground command and control center system integration. The successful accomplishment of these objective depends on the operational specifics of the onboard instrumentation, especially position sensors and communications links, but also on the capability of developing methodologies based on reliable and advanced basic research results. The present paper outlines some of these aspects, although not in an exhaustive manner, with particular reference to formation dynamic modeling, its stability and control, and automated guidance and navigation.

Increased performance in unmanned aerospace vehicles is leading toward mainly tailless new aerodynamic configurations for stealth capabilities, with perhaps high angles of attack for post stall aerodynamic regimes maneuverability, including thrust vectoring (agility, performance, and survivability following battle damage). In addiction, the use of multi-aircraft formations with remote control of a single or a few formation leader(s), with real time information exchange between the elements of the formation - supervised by some form of intelligent control - for higher levels of mission effectiveness is becoming increasingly appealing. The present effort is related to the latter aspect that is formation flying of unmanned air vehicles.

In the past, UAVs have been primarily used as test bed. They were used for instance to test flight envelope expansion, and flight control system for the manned aircraft or as a target for weapon systems. Over the past ten years, they have been envisioned as operational airborne platforms and have received considerable attention especially in many military strategic plans. From an engineering point of view, this was made possible and affordable in part by the miniaturization trend of flight control system components (sensors, actuators, CPUs, data acquisition systems, etc.), and by the increasing performance and speed of communication links.

The advantages of UAV technology appear several and clear. These vehicles, either flying in formation or individually, have high maneuverability potential, and in fact the only g-limitations are due to structural constraints because of the absence of a human pilot. In addition to eliminating the risk of human losses, UAVs have additional design advantages: a sophisticated cockpit is not required, no high redundant flight

Paper presented at the RTO AVT Course on "Intelligent Systems for Aeronautics", held in Rhode-Saint-Genèse, Belgium, 13-17 May 2002, and published in RTO-EN-022.

Report Documentation Page

Form Approved
OMB No. 0704-0188

1. REPORT DATE	2. REPORT TYPE	3. DATES COVERED
01 JUN 2003	**N/A**	**-**

4. TITLE AND SUBTITLE	5a. CONTRACT NUMBER
Intelligent Management Control for Unmanned Aircraft Navigation and Formation Keeping	5b. GRANT NUMBER
	5c. PROGRAM ELEMENT NUMBER
6. AUTHOR(S)	5d. PROJECT NUMBER
	5e. TASK NUMBER
	5f. WORK UNIT NUMBER
7. PERFORMING ORGANIZATION NAME(S) AND ADDRESS(ES) **Department of Electrical Systems and Automation University of Pisa, Via Diotisalvi 2, 56126 Pisa, Italy**	8. PERFORMING ORGANIZATION REPORT NUMBER
9. SPONSORING/MONITORING AGENCY NAME(S) AND ADDRESS(ES)	10. SPONSOR/MONITOR'S ACRONYM(S)
	11. SPONSOR/MONITOR'S REPORT NUMBER(S)

12. DISTRIBUTION/AVAILABILITY STATEMENT
Approved for public release, distribution unlimited

13. SUPPLEMENTARY NOTES
See also ADM001519. RTO-EN-022, The original document contains color images.

14. ABSTRACT

15. SUBJECT TERMS

16. SECURITY CLASSIFICATION OF:			17. LIMITATION OF ABSTRACT	18. NUMBER OF PAGES	19a. NAME OF RESPONSIBLE PERSON
a. REPORT	b. ABSTRACT	c. THIS PAGE			
unclassified	**unclassified**	**unclassified**	**UU**	**22**	

Standard Form 298 (Rev. 8-98)
Prescribed by ANSI Std Z39-18

control systems, and lower weight than a similar size manned aircraft. This could in turn be used, partially or fully, to increase the payload and/or the range. Another less apparent advantage is of a logistic nature and it is due to the fact that the deployment of UAVs can take place in very remote locations, without the need of deploying military rescue personnel in case a pilot rescue mission become necessary.

Operational potential of UAVs could strongly be improved in some cases by making them flying within a close formation. The first advantage comes from aerodynamic effects. It is well known in fact that aircraft with large aspect ratio wings have better overall aerodynamic efficiency because of reduction in drag for a given lift. However, large aspect ratio implies large wingspan for a given area, this means that the resulting structure will be unreasonably flexible and fragile for lightweight design. A similar improvement in overall efficiency can be achieved by flying multiple aircraft in close formation. In an idealized case of n identical aircraft, each with the aspect ratio AR flying in tip-to-tip formation, the effect would be that of a single aircraft with $nxAR$ aspect ratio. The aerodynamic benefits are due to favorable wake-vortex encounters. Wind tunnel tests and analytical studies have shown that the benefits increase as additional aircraft are added to the formation. Moreover, from an operational point of view, many aircraft involved in a mission can be better managed if they fly in a formation, rather than in an undefined structure.

An important challenge in the study of formation flight is represented by the complexity of the aerodynamic coupling. It is clear that the aerodynamic interference between different aircraft in the formation needs to be fully evaluated, modeled, and quantified since it may have critical effects on overall dynamic performances. For this purpose a primary factor is the size of the different aircraft within the formation; this, in turn, affects the aerodynamic interference induced by each one on the others of the formation, and, ultimately, dictates the relative distance allowed within the formation itself. Mathematical modeling of the aerodynamic interference between different aircraft in a formation was first approached by Bloy and others. They considered the problem of aerodynamic interference on lateral directional stability during air-to-air refueling maneuvers. In Reference [3], Myatt and Blake proposed an aerodynamic database with experimental data for the follower aircraft in a two-vehicle formation. In more recent studies, Gingras and co-workers proposed wind tunnel testing to acquire data for close vehicles simulation, while Nelson and Jumper used the Horseshoe Vortex theory to discuss the response of an airplane following an encounter with the trailing vortex wake by another. Blake, D'Azzo and Multhopp further discussed the problem of aerodynamic interference in a close formation flight, with a Leader/Wingman structure. The Leader generates vortices behind its wing. Such vortices exert actions on the Wingman lifting surfaces. In this approach, the Leader's wake is modeled via Horseshoe Vortex theory, and the drag reduction, sideslip force and induced angle of attack are introduced in the Wingman dynamics through additional stability derivatives leading to a mathematical aircraft model for a formation flight.

The other main challenge of close formation dynamics is the control system design. Close formation flight control, intended in its broad aspects of guidance, navigation and control, was originally studied for a classic leader/wingman configuration. An aircraft (Leader) is selected to direct the formation, following a prescribed path, and all the others (Wingmen) are expected to maintain a fixed relative distance with respect to the lead airplane, in order for the formation to have a desired geometrical shape. D'Azzo and co-workers analyzed the kinematical coupling effect of a two-aircraft configuration, and introduced a proportional integral (PI) controller for formation control. Wolfe, Chichka, and Speyer introduced the concept of decentralized control for UAVs in formation flight in reference 11. The advantages of using decentralized controllers are clear, especially for a large size UAVs formation, a full state feedback solution for the problem could be quite unfeasible due to the very high number of states. In addition, a decentralized control approach would provide more flexibility for time-varying number of UAVs in the formation. Later work by Chichka, Speyer, Chichka, Speyer, and others, in references 11 and 12 respectively, focused on a peak seeking control approach for close formation flight where the overall formation control was approached as an optimal control problem with the objective of minimizing the overall drag. A fairly intensive and inclusive study on formation flight control - with the use of a PI control scheme- was presented by Proud, Pachter, and D'Azzo for a 2-D formulation of the problem, and then recently extended to a 3-D formation dynamics problem. Schumacher and Kumar recently presented results on the use of adaptive control within the area of formation control. This adaptive scheme featured an optimal LQR design for the outer loop and a Dynamic Inversion design for the inner loop.

The paper is structured as follows: In the next section some classical approaches to formation dynamics and control are presented. Then, a procedure for aerodynamic interference is suggested, in order to improve the aircraft models. Given a lifting surface system, the proposed technique permits the calculation of induced velocities and then the forces due to coupling effects between aerodynamic surfaces. Simulation results with a three-aircraft formation have shown that each aircraft experiences an increase in lift and a drag reduction by

flying in a close formation. This result does not appear if a single Horse-Shoe Vortex technique were used, because such method is based on the hypothesis that only the follower is affected by the wake. Thus, the above results are used to obtain the dynamic model of an aircraft flying within a formation. A different approach to formation flight is presented where each aircraft does not refer to the preceding one or to the formation leader, but keeps its position with respect to an imaginary point in the formation whose dynamics depend on all the others. The approach is based on the apparent behavior of some migratory birds, that during flight 'wait' for the those birds which have changed the original geometry of the formation by flying in a different path. The formation controller is constituted by two subsystems: a trajectory controller which provides tracking of a prescribed path, and a position controller which permits formation geometry keeping. These control laws are mixed by a parameter that depends on the position error. Finally, a waypoint-based guidance scheme is suggested as a potentially appropriate navigation loop.

Traditional Formation Control

The formation control problem can be traditionally approached, by designing first an inner loop, that allows tracking commanded velocity, altitude and heading. The outer loop consists of a Formation Controller (FC) that generates a reference path command for the inner loop, in order to follow a desired trajectory and to maintain the formation geometry.

The basic dynamic model for inner loop controller design, has a standard linearized form given by

$$\begin{cases} \dot{x} = Ax + Bu \\ y = Cx + Du \end{cases}$$

with $x \in \Re^n, y \in \Re^p, u \in \Re^m$ as state, output and input vectors respectively. In particular, we refer to a sample trim condition corresponding to *Mach* = 0,4 and altitude of 10,000 *ft*. The dynamics described above include four inputs (symmetrical and differential taileron deflection, rudder deflection and engine throttle, and 14 states inclusive of 6 body rates, Euler angles, center of mass position and engine states.

Inner Loop Synthesis

Assuming dynamic separation between longitudinal and lateral-directional modes, the state and control vectors can be partitioned as follows

$$\begin{cases} \dot{x} = \begin{bmatrix} \dot{x}_{long} \\ \dot{x}_{lat} \end{bmatrix} = \begin{bmatrix} A_{long} & 0 \\ 0 & A_{lat} \end{bmatrix} x + \begin{bmatrix} B_{long} \\ B \end{bmatrix} \begin{bmatrix} u_{long} \\ u_{lat} \end{bmatrix} \\ y = \begin{bmatrix} y_{long} \\ y_{lat} \end{bmatrix} = Cx + Du \end{cases}$$

An LQ-Servo system was developed, shown in Figure 1 with the longitudinal inner-loop controller based on the above and capable of providing adequate tracking of commanded velocity and altitude.

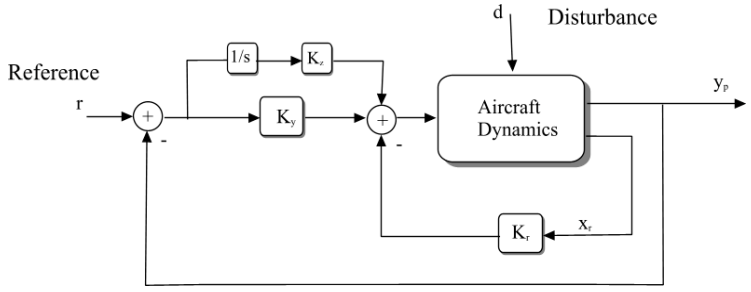

Figure 1. LQ-Servo Block Diagram

the full state feedback gain matrix K_{long} was obtained from the solution of the algebraic Riccati equation associated to the quadratic cost function in

$$\int_0^\infty \left(y_{long}^T Q y_{long} + u_{long}^T R u_{long} \right) dt$$

where

$$y_{long} = \begin{bmatrix} u & w & q & \theta & h \end{bmatrix}^T , u_{long} = \begin{bmatrix} \delta_e & \delta_{th} \end{bmatrix}^T . \text{ with}$$

$$\begin{cases} u_{long} = -K_{long} x_{long} & A_{ong}^T P_{long} + P_{long} A_{long} + C_{long}^T Q C_{long} \\ K_{long} = R^{-1} B_{long}^T P_{long} & -P_{long} B_{long}^T R^{-1} B_{long} P_{long} = 0 \end{cases}$$

The lateral-directional inner loop was synthesized in a fashion similar to the longitudinal one. The full state feedback controller is given by

$$u_{lat} = -K_{lat} x_{lat}$$

and the gain matrix K_{lat} is obtained with a minimization of a performance index such as the one above. Tracking is achieved as shown in Figure 2 below, and more detailed results can be found in [9].

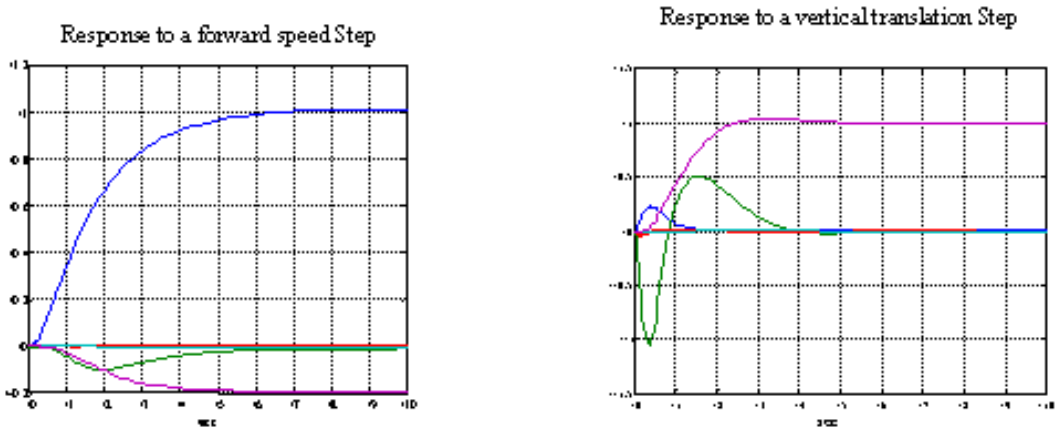

Figure 2. Inner Loop Controller Performance

Formation Control

In a typical formation flight, the Wingman follows the trajectory of the Leader, taking the other aircraft as reference to keep its own position inside the formation. In a large, rigidly flying formation, intra-aircraft distances must be kept constant. Then formation trajectory definition is usually the primary responsibility of the Leader. Many important aerodynamic effects influence the specifications of the overall control system, such as the vortex leaving the trailing edge of the wing for instance. In order to attain a more realistic simulation of a formation, a horseshoe vortex model of a wake was introduced. To simplify the calculation of the induced velocities, the tail creates no vortices, under the assumption that the main wing lifting effect is much larger. The vortex produces an up-wash on the wing of the following aircraft. The main up-wash effect is the increase of angle of attack, with respect to the isolated flight condition, thus more lift is generated. The vortex-induced velocity decreases with distance; hence the left side of the wing will be more affected than the right side. This causes a rolling moment, thus an attitude automatic control is necessary. Creation of a yawing moment has been neglected due to its weak contribution.

The primary objective of the formation controller (FC), also based on LQR techniques, is to maintain the formation geometry. To compute the distance to its reference, each aircraft acquires its position $P = (X, Y, H)$ from a GPS-based position sensing system, and receives, through appropriate communication channels, other aircraft positions $P_R = (X_R, Y_R, H_R)$. The formation controller is also responsible for having each aircraft follow a prescribed path. Each FC receives path information in terms of velocity, heading and altitude $T_R = (V_R, H_R, \psi_R)$, from another Wingman, the Leader or a ground station. Then the received data vector becomes $R_R = (X_R, Y_R, H_R, V_R, \psi_R)$. The commanded trajectory for the inner loop controller can be defined then as $T_C = T_R + \Delta T$, where ΔT is the output of the formation controller. The position error inside the formation is $\Delta P = P_R - P$, and it is composed of the error in the formation plane $\Delta P_{XY} = [\, X_R\text{-}X,\ Y_R\text{-}Y \,]$ and error in the vertical plane $\Delta P_H = [\, H_R\text{-}H \,]$: $\Delta P = [\, \Delta P_{XY},\ \Delta P_H \,]$. These coordinates come from two GPS receivers, and are expressed in an earth fixed reference frame; they must be rotated into the aircraft body-fixed frame: $\Delta P' = [\Delta P'_{XY},\ \Delta P'_H \,]$ using aircraft Euler angles $[\phi, \theta, \psi\,]$ in order to be used by the formation controller. In fact, only ΔP_{XY} must be rotated in order to keep the formation in the X-Y plane, otherwise $\Delta P'_H$ would depend on the (ϕ) or pitch (θ); then $\Delta P'_H = \Delta P_H$, and

$$[\Delta P'_{XY},\ 0] = {}^{B}R_E(\phi, \theta, \psi) \cdot [\, \Delta P_{XY},\ 0 \,]$$

where ${}^{B}R_E$ is the earth-to-body frame rotation matrix. The effective formation controller was designed with linear quadratic control techniques and takes $\Delta P'$ as input. Figure 3 shows the complete control block diagram. The resulting control law is:

$$\Delta T = K_{FC}(s)\Delta$$

The FC applies the corrections ΔT to the reference trajectory T_R to generate trajectory commands T_C for the aircraft autopilots. These corrections take into account the changes in velocity, heading and altitude, to the reference trajectory, that are necessary to maintain the formation geometry. Each aircraft can take more than one reference from the other elements of the formation. A convex combination ΔP_W of the distance errors ΔP_i, from the *i-th* aircraft taken as reference, can be used as a unique position error by the formation controller as:

$$\Delta P_W = \sum_{i=1}^{m} k_i \Delta P_i \qquad \sum_{i=1}^{m} k_i = 1 \qquad k_i > 0 \quad \forall i$$

Using ΔP_W, in place of ΔP, allows the formation to possess a certain degree of "elasticity"; that is, the formation stretches in the direction of keeping the average position error to a minimum.

To validate the overall control system performance, several computer simulations were performed with a three-aircraft diagonal formation shown in Figure 4. The relative nominal distances between each aircraft were set to be 15 and 10 meters along the x and y-axis respectively while the altitude was the same for all. With respect to the sequential references chain, two types of simulations were performed with two different strategies:

Leader Mode: Both Wingman1 and Wingman2 take the trajectory references from the Leader of the formation.

Front Mode: Each aircraft takes its reference from the preceding one. In this case, Wingman1 is referred to Leader and Wingman2 is referred to Wingman1.

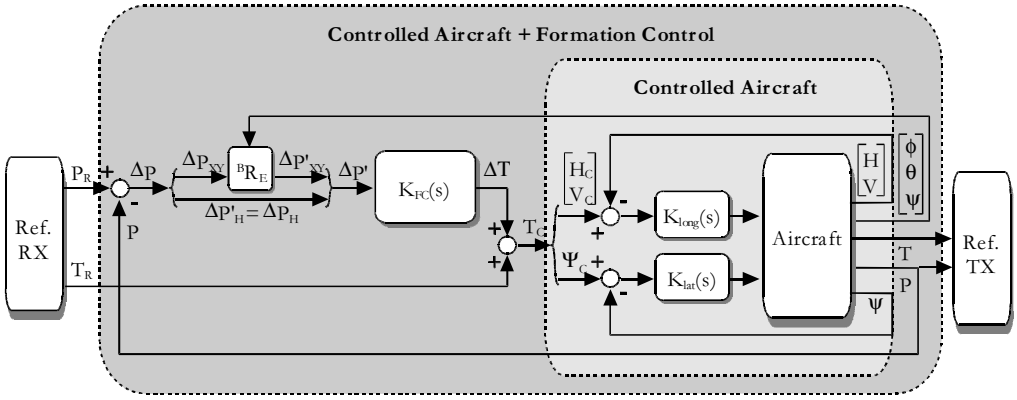

Figure 3. Complete control scheme.

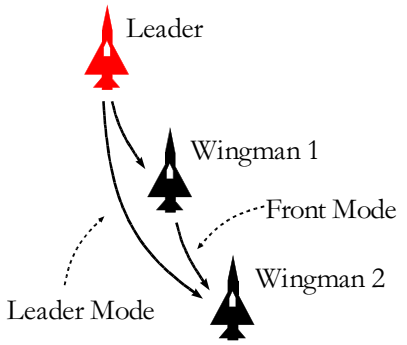

Figure 4. Three aircraft diagonal formation geometry**.**

Figures 5 and 6 show the responses of the Wingman2 to airspeed and altitude commands in Leader Mode and Front Mode. In the Front Mode structure, Wingman2 presents a poorer transient response, due to error propagation. Although no optimized synthesis was performed in the computation of the control gains, and each vehicle posts the same set of gains, on the basis of the preceding simulation results a formation controller based on Leader Mode suggests better transient responses because of the absence of error propagation along the references chain. On the other hand, this type of formation structure may be more critical, because in this case, Wingman2, which is directly connected to the Leader, has no information about its distance to Wingman1 therefore it would be not capable of avoiding a collision with Wingman1. Optimizing the autopilot, which is not the focus of the present work, can reduce error propagation.

Improved Strategy for Formation Control

In this section we present a more accurate dynamic modeling, and a modified formation controller structure. A traditional single Horseshoe Vortex technique consists in replacing the whole lifting surface by single vortex made with two free segments and one wing-fixed segment. Such model is simple and introduces minor modifications to the dynamics equations. However, by modeling a Leader/Wingman close formation by the single Horseshoe Vortex theory, only one aircraft is affected by the wake efforts, and the effect of the wake along the *x*-axis is not modeled to obtain a close analytical solution. This may cause the results not to be very accurate or complete.

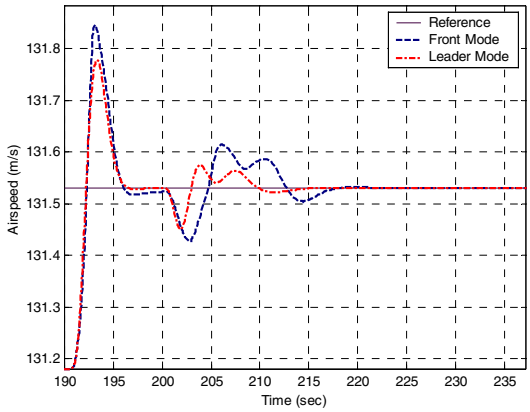

Figure 5. Wingman2 response to speed command.

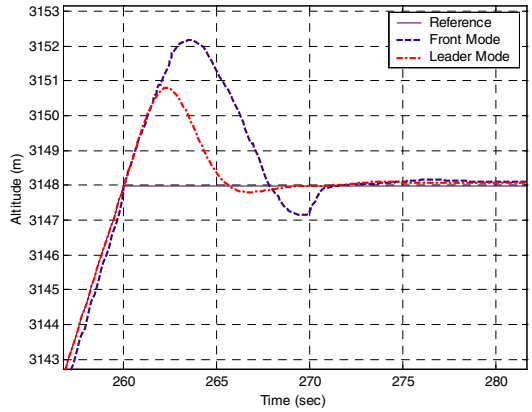

Figure 6. Wingman2 response to an altitude command.

In fact, in a formation flight problem, the mathematical modeling for all the aircraft involved in the formation is a critical issue. On the other hand, experimental data from wind tunnel tests could describe completely the aerodynamics interference effects but may become too costly in case of an increasing number of vehicles. Here, a different 3-D approach, based on a wing-distributed Horseshoe vortex system is presented. Given a system of lifting surfaces, this technique features the calculation of induced velocities as well as the forces and moments due to the coupling effects between all the aerodynamics surfaces. The first step consists in defining the lifting surfaces, only single tapered wings are considered here. To define each lifting surface, the following vector containing geometrical and aerodynamic parameters of the root profile is introduced:

$$R_p = \left[\delta_h \quad \Lambda \quad \sigma \quad c_r \quad c_t \quad C_{L_\alpha} \quad C_{m_0} \quad \alpha_\infty \right]$$

Once a number *s* of lifting surfaces has been defined, each surface is modeled through a straight line, also known as *lifting line*, passing through the aerodynamic center of the local profile. The aerodynamic center of the single profile is approximately set at 26% of the geometric chord. Let us now consider the *r- th* lifting surface. First the two halves of its lifting line are divided in *nr*/2 segments, then a vortex system, composed by a number *nr* of horseshoe vortices, is distributed on each lifting line. Each horseshoe vortex is modeled with a wing-fixed portion and two free portions that extend to infinity. Thus the two following subsets of points are introduced:

$$P_r = \left\{ P_{k_r} \in \mathbb{R}^3;\, k = 1 \ldots n_r + 1 \right\}$$

$$m_r = \left\{ m_{k_r} \in \mathbb{R}^3;\, k = 1 \ldots n_r \right\}$$

The first subset P_r contains the points where the free portions of each horse-shoe vortex leaves the lifting line. The second subset m_r contains the points where the induced velocity is evaluated. They are the middle points of the wing-fixed portions of each horse-shoe vortex. Figure 7 shows, as an example, the generic *r- th* lifting surface with the vortex system along with the points P_{kr} and m_{kr} .

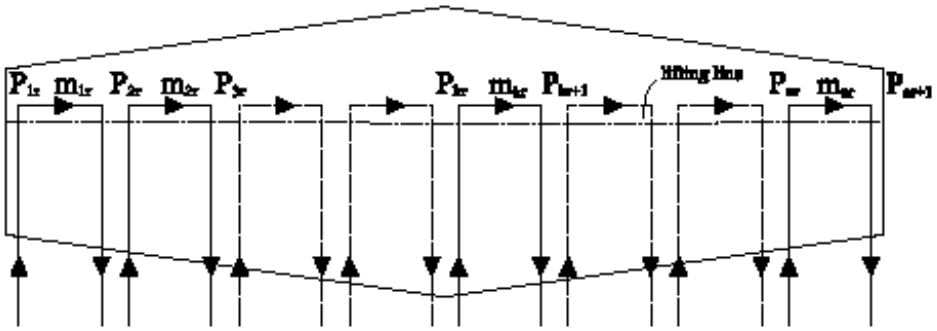

Figure 7. Lifting surface and vortex system

Once the lifting surfaces have been defined, in terms of lifting line and vortex systems, the induced velocity and then the strength of the vortices may be evaluated. The aerodynamic interference is calculated by locally using the fluid dynamic analogue of the Biot-Savart law from electromagnetism. Such law is applied both to the wing-fixed portion and to the free portions of each vortex yielding the computation of the vortex system strength. At this point, aerodynamic forces, moments, and coefficients can be calculated, which for a conventional air vehicle can be expressed as:

$$C_{F_1} = \sum_{t=1}^{3} C_{F_t}, \ldots, C_{F_{n_a}} = \sum_{t=s-2}^{s} C_{F_t}$$

$$C_{M_1} = \sum_{t=1}^{3} C_{M_t}, \ldots, C_{M_{n_a}} = \sum_{t=s-2}^{s} C_{M_t}$$

for a n_a aircraft formation. Aerodynamic calculations were performed for a close formation, consisting of three unmanned aircraft systems. The relative nominal distances between aircraft were chosen to be 4 and 5 m along the *x and y* respectively, with the altitude held constant. The geometries of the close formation are shown in Figure 8. Aerodynamic and geometry data used for this calculations are listed in Table 1, while the evaluated force and moments coefficients, for the formation configurations based on the previous data are provided in Table 2, compared to the values for 'isolated' flight. From the results it can be seen that the rear aircraft gain an increase in lift and an induced drag reduction by flying in formation. It is also important to notice that the front aircraft has an increase in lift coefficient and a drag reduction compared to solo flying. This last result is not found by using simple horseshoe wake models.

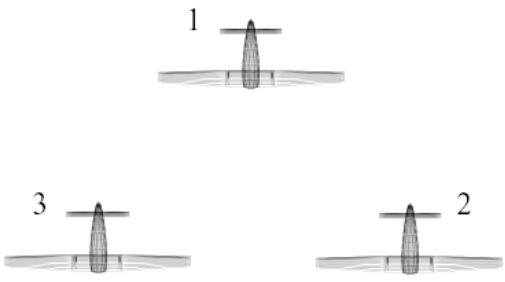

Figure 8. Formation geometry for Wake contribution evaluation

Parameter	Value
Wing area, S, m^2	0.697
Wing span, b, m	3.0
Tail span, b_t, m	1.1
Vertical tail height, h_v, m	0.25
Wing root cord, c_r	0.28
Wing tip cord, c_t	0.16
Tail root cord, c_r	0.12
Tail tip cord, c_t	0.06
Vertical tail root cord, c_r	0.22
Vertical tail tip cord, c_t	0.12
Root lift curve slope, $C_{L_a}, 1/rad$	5.878
Root tail curve slope, $a_t, 1/rad$	5.878
Root vertical tail curve slope, $a_{v_t}, 1/rad$	5.878

Table 1: Aerodynamic data

Aerodynamic	Isolated	Formation Flight		
Coefficients	flight	1	2	3
C_{x_i}	0.022346	0.022796	0.023635	0.023635
C_y	0	0	-0.000066	-0.000066
C_z	-0.672993	-0.676335	-0.682787	-0.682787
C_l	0	0	-0.000781	0.000781
C_m	0.133341	0.133068	0.132804	0.132804
C_n	0	0	-0.000109	0.000109

Table 2: Close formation evaluated coefficients (body axis)

Formation Dynamics

In this section, the mathematical model of an aircraft flying within a formation is outlined. The main difference with respect the model of an 'isolated' aircraft consists in the value of the aerodynamic coefficients. The modeling procedures outlined before are introduced. Once the mathematical model is developed, the kinematic equations describing the relative distances between the aircraft are presented. These equations are the basis of formation control system design. The aerodynamic force and moment coefficients can then be directly introduced in the flight dynamic equations. However, is useful to split the aerodynamic coefficients according two different contributions:

$$\begin{pmatrix} C_F \\ C_M \end{pmatrix} = \begin{pmatrix} C_{Fi} \\ C_{Mi} \end{pmatrix} + \begin{pmatrix} C_{Ff} \\ C_{Mf} \end{pmatrix}$$

The first term on the right hand side of the previous equation is the coefficient in case of 'isolated' flight, while the second is related to the contributions associated with formation flying. This can be useful within the design of the control laws, since the wake effects can be treated as disturbances to be rejected by the control system.

The basic model used here is a 3DOF dynamic system shown below, with standard notation:

$$\begin{aligned}\dot{V} &= \frac{(T-D)}{m} - g\sin\gamma \\ \dot{\gamma} &= \frac{g}{V}(n\,\cos\phi - \cos\gamma) \\ \dot{\chi} &= \frac{g\,n\sin\phi}{V cos\gamma}\end{aligned}$$

The state variables describing the aircraft dynamics are the airspeed V , the flight path angle γ and the heading angle χ, while T, n and ϕ, are thrust, load factor and bank angle and they are the input variables; D is the aerodynamic drag and m the aircraft mass. According to the aerodynamic coefficients separation, the system can be rewritten introducing changes in lift, induced drag and side force. This leads to:

$$\dot{V} = \frac{T-D}{m} - g\sin\gamma - \frac{\Delta D_{\boldsymbol{i}}}{m} \quad \dot{\gamma} = \frac{g}{V}\left[(n + \frac{\Delta L}{mg})\,\cos\phi - \cos\gamma\right] \quad \dot{\chi} = \frac{g(n+\frac{\Delta L}{\boldsymbol{mg}})\sin\phi}{V\cos\gamma} + \frac{\Delta Y}{mV}$$

or, in compact form

$$\dot{\boldsymbol{X}}_{\boldsymbol{f}} = \dot{\boldsymbol{X}}_{\boldsymbol{i}} + \frac{1}{2}\rho V^2 S\left(\boldsymbol{\Delta}_{\boldsymbol{f}} \cdot \boldsymbol{C}_{\boldsymbol{Ff}}\right)$$

$$\boldsymbol{\Delta}_{\boldsymbol{f}} = \begin{pmatrix} 1/m & 0 & 0 \\ 0 & \cos\phi/mV & 0 \\ 0 & \sin\phi/(mV\cos\gamma) & 1/mV \end{pmatrix}$$

To maintain the formation geometry, each aircraft must keep its prescribed distance from a reference. Such reference may be the Leader of the formation or a neighborhood aircraft or an imaginary point within the formation. To calculate the relative distance of the *i-th* aircraft from its reference *r*, three reference frames are introduced: an inertial, Earth-Fixed frame F_O and two kinematic frames F_{ki} and F_{kr}, with the origin on aircraft *i ¡ th* and on reference *r* respectively. The relationship between position derivatives in the variuos reference frames is given by

$$\dot{\boldsymbol{P}}_{\boldsymbol{r}}^{\boldsymbol{O}} = \dot{\boldsymbol{P}}_{\boldsymbol{i}}^{\boldsymbol{O}} + \boldsymbol{V}_{\boldsymbol{i,r}}^{\boldsymbol{O}} + \boldsymbol{\Omega}_{\boldsymbol{i}}^{\boldsymbol{O}} \times \boldsymbol{R}_{\boldsymbol{i,r}}^{\boldsymbol{O}}$$

$$\boldsymbol{V}_{\boldsymbol{r}}^{\boldsymbol{i}} = \boldsymbol{V}_{\boldsymbol{i}}^{\boldsymbol{i}} + \boldsymbol{V}_{\boldsymbol{i,r}}^{\boldsymbol{i}} + \boldsymbol{\Omega}_{\boldsymbol{i}}^{\boldsymbol{i}} \times \boldsymbol{R}_{\boldsymbol{i,r}}^{\boldsymbol{i}}$$

with

$$\boldsymbol{V}_{\boldsymbol{r}}^{\boldsymbol{i}} = \begin{bmatrix} V_r\cos\gamma_e\cos\gamma_e \\ V_r\cos\gamma_e\sin\chi_e \\ -V_r\sin\gamma_e \end{bmatrix} \quad \begin{bmatrix} \dot{dx} \\ \dot{dy} \\ \dot{dz} \end{bmatrix} = \begin{bmatrix} V_r\cos\gamma_e\cos\gamma_e \\ V_r\cos\gamma_e\sin\chi_e \\ -V_r\sin\gamma_e \end{bmatrix} - \begin{bmatrix} V_i \\ 0 \\ 0 \end{bmatrix} + \begin{bmatrix} \dot{\gamma}_i dy - \dot{\chi}_i dz \\ -\dot{\chi}_i dx \\ \dot{\gamma}_i dx \end{bmatrix}$$

$$\gamma_e = \gamma_r - \gamma_i \text{ and } \chi_e = \chi_r - \chi_i.$$

The previous method for relative distances calculation is typically used when, during the mission, aircraft within the formation exchange each others trajectory information, particularly airspeed, flight path angle, and heading angle. If the trajectory information are not available, and the if aircraft could know only the absolute

position (e.g. by GPS), the relative distances between aircraft could be computed first referred to the inertial frame and then rotated to the kinematic frame of each aircraft.

Formation Strategy

The Leader/Wingman structure may not be the best strategy to perform complicated maneuvers, especially in multi-aircraft formation flight. In fact, each aircraft in the formation must cooperate in order to maximize the possibilities for a formation to obtain and retain its structure. The aircraft in the formation must work together to achieve a common goal; then, to overcome the limitations of Leader/Wingman structure, a different strategy is proposed, based on the behavior of migrational birds. The aircraft in a formation are not longer referring to each other, but they are required to keep a specified distance from an imaginary point called Formation Geometry Center (FGC). The FGC position depends on the relative distances between the aircraft in the formation itself; this allows each aircraft to have the capability of sensing other vehicles movement from the nominal position in the formation. In the presence of disturbances, for instance, if one of the aircraft loses its position, the other senses the change, and depart momentarily from the prescribed trajectory, manoeuvreing all-together in order to reconstitute the formation geometry. Once the geometry has been reached again, all aircraft continue to follow the prescribed trajectory. This approach is typical of several species of migrational birds.

For long distance migrational flight, birds of several species tend to move in a formation, flying close to each other maintaining a defined geometrical shape. One of the most interesting considerations is the fact that during a migrational flight if one or more elements of the group loses its position in the formation, the others leave the migration trajectory and 'wait' for the lost ones until the formation shape is reconstituted. There are two main reasons why birds fly in a formation; the first reason is related to aerodynamic considerations while the other is due to the 'social behavior' of some species of birds. In terms of aerodynamics effects, birds take advantage of the induced velocity produced by the wing tip vortex phenomenon: the inner wing of each bird in a V formation, for example, gains an increase in lift and then a reduction in induced drag from the upward rising side of the vortex left by the outer wing of the bird ahead. For this reason, it is important that each bird in the group keeps its position; losing position by one or more birds in a migrational flight means to lose a non-negligible portion of aerodynamics efficiency. On the other hand, birds like geese and swans form 'family' groups: offspring remain with parents one or two seasons after the birth and fly together with them during the migration. The elements in these formations know each other and try to remain together independently from aerodynamics advantages while other birds like storks live in non-familiar group, but fly together with others just in order to improve the efficiency of the migration (especially during food searching or meeting season). From these motivations it's possible to assume that the preceding consideration to be reasonable. A two-aircraft formation is considered in the present work. Each aircraft in the formation will be represented using the modified three-degrees of freedom point-mass model described in the previous section.

In this approach, aircraft do not refer to each other and, in order to maintain formation geometry an imaginary point called Formation Geometry Center (FGC) is introduced and each aircraft must keep a prescribed distance from this point. The FGC dynamics for an *N*-aircraft formation can be represented by the following differential equations:

$$\begin{aligned} \dot{x}_{FGC} &= \sum_{i=1}^{n_a} \frac{V_i \cos\gamma_i \cos\chi_i}{n_a} \\ \dot{y}_{FGC} &= \sum_{i=1}^{n_a} \frac{V_i \cos\gamma_i \sin\chi_i}{n_a} \\ \dot{z}_{FGC} &= \sum_{i=1}^{n_a} \frac{-V_i \sin\gamma_i}{n_a} \end{aligned}$$

By integrating the preceding equations, the position of the FGC in the Earth-fixed frame (P_{FGC}) is found and the distance between the FGC and the *i-th* aircraft, referred to the frame F_O, is defined as:

$$\boldsymbol{d}_i = \boldsymbol{P}_{FGC} - \boldsymbol{P}_i$$

Prior to the design of any formation controller, each aircraft of the formation must feature adequate tracking of a commanded trajectory through an inner loop controller. The innerloop controller is based on the model for an individual aircraft in undisturbed air described in the previous section. The following three lag filters are introduced to model the fact that the aircraft cannot change bank angle (ϕ), load factor (n) or thrust (T) instantaneously.

$$\dot{T} = (T_c - T)/\tau_t$$

$$\dot{\phi} = (\phi_c - \phi)/\tau_b$$

$$\dot{n} = (n_c - n)/\tau_n$$

To implement the inner-loop controller, a dynamic inversion law is used. The desired trajectory vector is written in terms of a commanded airspeed (Vc), flight path angle (γ), and heading angle (χ). It is assumed that the desired trajectory will be governed by the following linear time-invariant equations:

$$\dot{\gamma} = \omega_\gamma(\gamma_c - \gamma)$$

$$\dot{V} = \omega_V(V_c - V)$$

$$\dot{\chi} = \omega_\chi(\chi_c - \chi)$$

The bandwidth dictates how quickly the actual aircraft trajectory changes with respect to the new desired value. To derivate the dynamic inversion control law, the commanded rates are set equal to the associated actual, and then solving for thrust, bank angle, and load factor. The computed thrust, bank angle, and load factor become the commanded values needed and are given by:

$$T_c = D + \omega_v(V_c - V)m + mg\sin\gamma$$

$$n_c\cos\phi_c = \frac{V}{g}\left[k_\gamma\left(\gamma_c - \gamma\right) + \cos\gamma\right] = c_1$$

$$n_c\sin\phi_c = \frac{V}{g}k_\chi\left(\chi_c - \chi\right)\cos\gamma = c_2$$

from which

$$n_c = \sqrt{{c_1}^2 + {c_2}^2}$$

$$\phi_c = tan^{-1}\left(\frac{c_2}{c_1}\right)$$

Once the autopilot structure is defined as above, the model for a *N*-aircraft formation is obtained by introducing the force coefficients variations and the relative distances dynamics:

$$\begin{aligned}
\dot{\boldsymbol{x}}_1 &= f_1(\boldsymbol{x}_1, \boldsymbol{u}_1) + \tfrac{1}{2}\rho V_1^2 S_1 \left(\boldsymbol{\Delta}_{f_1} \cdot \boldsymbol{C}_{F_1 f}\right) \\
&\dots \\
\dot{\boldsymbol{x}}_n &= f_2(\boldsymbol{x}_n, \boldsymbol{u}_n) + \tfrac{1}{2}\rho V_n^2 S_n \left(\boldsymbol{\Delta}_{f_n} \cdot \boldsymbol{C}_{F_n f}\right) \\
\dot{\boldsymbol{d}}_1 &= g_1(\boldsymbol{x}_1, \dots, \boldsymbol{x}_n) \\
&\dots \\
\dot{\boldsymbol{d}}_n &= g_n(\boldsymbol{x}_1, \dots, \boldsymbol{x}_n)
\end{aligned}$$

A Formation Controller (*FC*) is needed to reproduce the natural behavior of migrational birds. For the purpose of *FC* design, linearization around a selected flight condition of the above nonlinear model yields the linearized set of equation described by the following standard state space model:

$$\begin{cases} \dot{x} &= Ax + Bu \\ y &= Cx \end{cases}$$

Each aircraft has its *FC* constituted by two control systems: trajectory controller (*KT*) and position controller (*KP*). The main objective of the trajectory controller is to provide tracking of a prescribed path in terms of desired velocity, flight path and hading angle, while the position controller is designed to maintain inter-aircraft distances in order to give the formation a desired geometric shape. Trajectory and position controllers receive path error information, that is the difference between current and desired path, and FGC-distance error, that is the difference between current and desired distance from FGC, respectively:

$$\begin{aligned} e_T &= r_T - y_T \\ e_P &= r_P - y_P \end{aligned}$$

and they generate trajectory and position commanded vectors defined as:

$$\begin{aligned} u_T &= K_T e_T \\ u_P &= K_P e_P \end{aligned}$$

An LQ-Servo controller was developed, and gain matrices K_T and K_P were obtained through the minimization of the quadratic cost indexes:

$$J_{(\cdot)} = \int_{t_0}^{\infty} \left[u'\, R_{(\cdot)}\, u + e'_{(\cdot)}\, Q_{e(\cdot)}\, e_{(\cdot)} + \right.$$

$$\left. + x'_{r(\cdot)} Q_{r(\cdot)} x_{r(\cdot)}\right] dt$$

where Q_e regards the minimization of the desired output vector, while Q_r is related to the residual state vector. The resulting commanded vector *uc* is a convex combination of the two previous control laws:

$$u_c = (1 - f)u_T + f u_P$$

where $f \in [0; 1]$, is a function of the position error e_P. The prescribed path can be commanded by one of the aircraft of the formation or by a ground station o by a Virtual Leader. In the presence of disturbances, there may be one or more aircraft with a position error with respect to the nominal configuration. In this case, the command vector u_C depends both on position error e_P and trajectory error e_T and so the aircraft in the formation may not be able to follow the prescribed path exactly until the geometry is re-established. When the formation has the desired shape, the position error e_P is zero for each aircraft and f=1. This causes the commanded vector be given only by the contribution of the trajectory controller and all the aircraft will follow the desired trajectory r_T.

Simulation Results

To validate the overall control strategy, simulations were performed for close formations consisting of two aircraft. The aircraft model includes aircraft/autopilot, the distributed HorseShoe Vortex code and *FGC* relative distance dynamics.

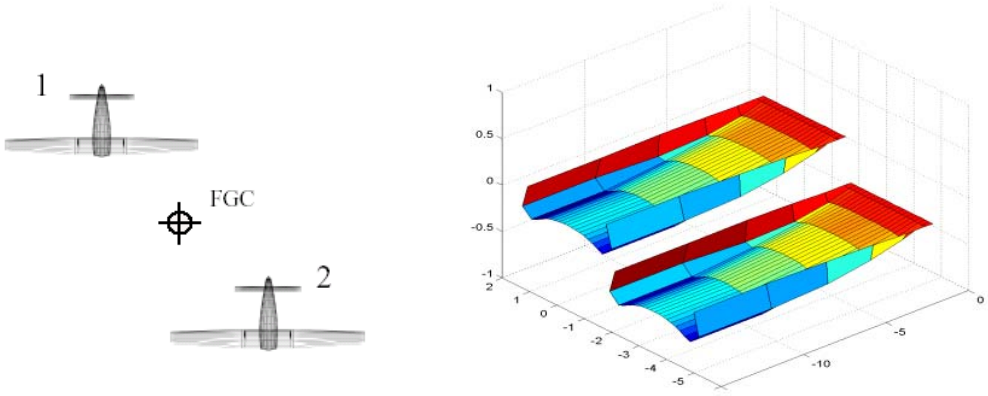

Figura 9. Two-aircraft configuration for simulation

The whole Formation Control scheme for such formation is shown in Figure 10 and is simulated in a MATLAB environment. The relative nominal distances between aircraft and *FGC* are selected to be 5 m along the *x* and *y* axes. The altitude is the same for both aircraft at 300m.

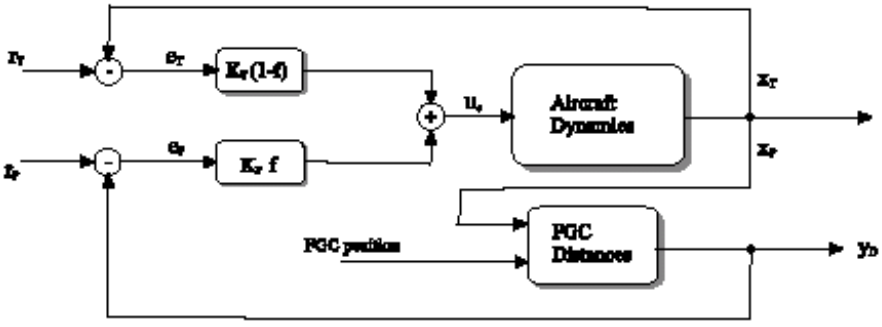

Figure 10. Complete formation controller for a Two-aircraft configuration

Additional aircraft data required for this effort are listed in Table 3 and the evaluated aerodynamic coefficient variations for this formation structure are listed in Table 4.

Parameter	Value
Velocity time constant, ω_V, s	0.3
Flight path time constant, ω_γ, s	0.2
Heading time constant, ω_χ, s	0.2
Thrust time constant, τ_t, s	0.9
Load factor time constant, τ_n, s	0.5
Bank angle time constant, τ_b, s	0.5
Gross mass, m, kg	10
Velocity, $V_\infty, m/sec^2$	20
Air density, $\rho, kg/m^3$	1.219

Table 3: Aircraft value for control design

Aerodynamic Coefficients	Aircraft 1	Aircraft 2
$\mathbf{\Delta} C_{D_i}$	-0.0015	-0.0020
$\mathbf{\Delta} C_Y$	-0.000004	0.000078
$\mathbf{\Delta} C_L$	0.0214	0.0297

Table 4: Evaluated force coefficient variations

The first simulation a path following task. Each aircraft receive the commanded trajectory from the VL. Starting from a steady-level flight condition at 20 m/sec, each aircraft is commanded to perform a heading change of -30 deg. Trajectory tracking is achieved and the relative distances between the aircraft are maintained at nominal values. Figure 11 shows aircraft response to the heading command, while Figure 12 shows the relative distance between aircraft and the *FGC* during the same manuever.

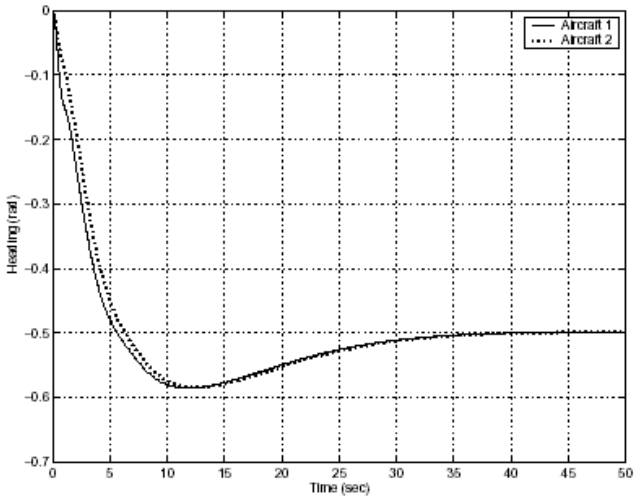

Figure 11. Aircraft responses to a 30 deg. Heading change

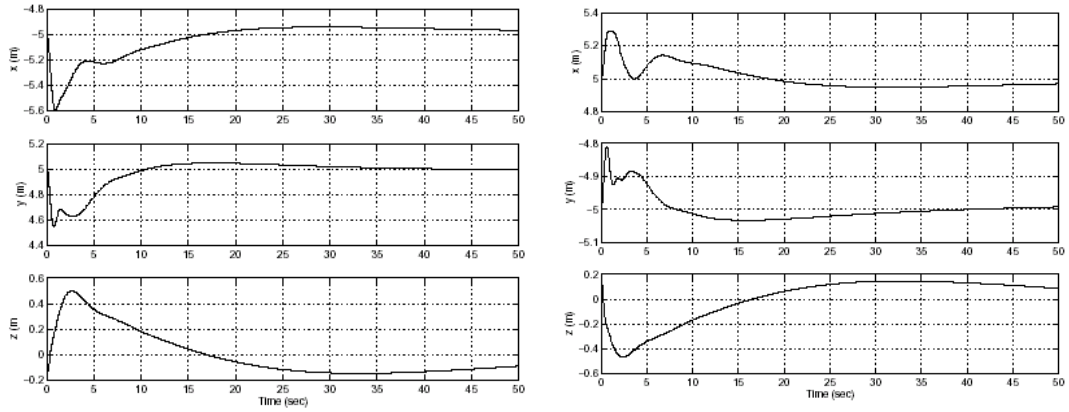

Figure 12. Relative distance of the two aircraft from *FGC*.

The second simulation is related to a formation geometry variation. Each aircraft is commanded to increase its relative distances from *FGC* from 5 to 7 m along *x* and *y*-axis. Figure 13 shows the relative distance between aircraft and the *FGC* while Figure 14 shows the airspeed time history during such maneuver.

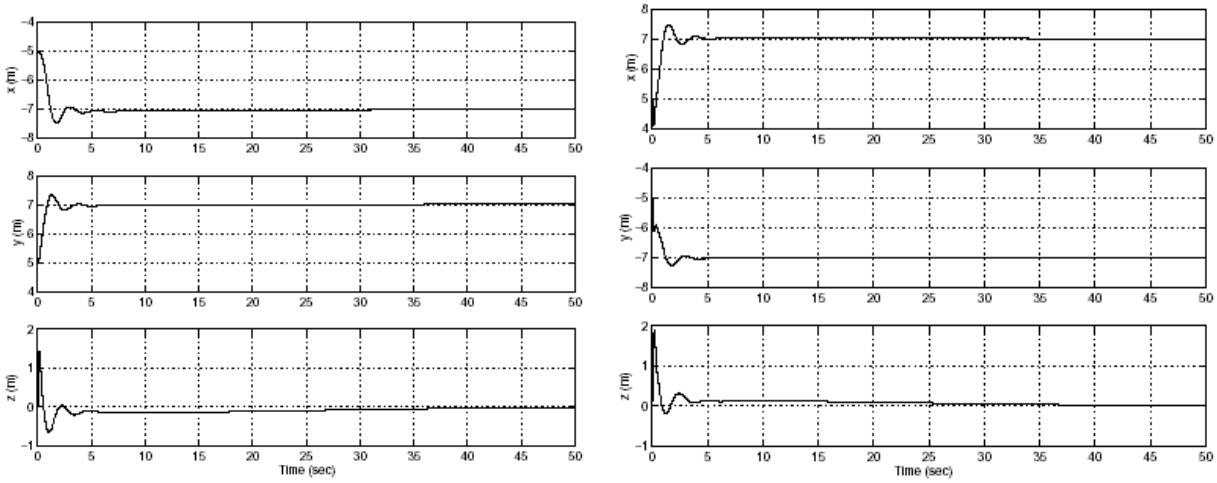

Figure 13. Relative distance of the two aircraft from *FGC*.

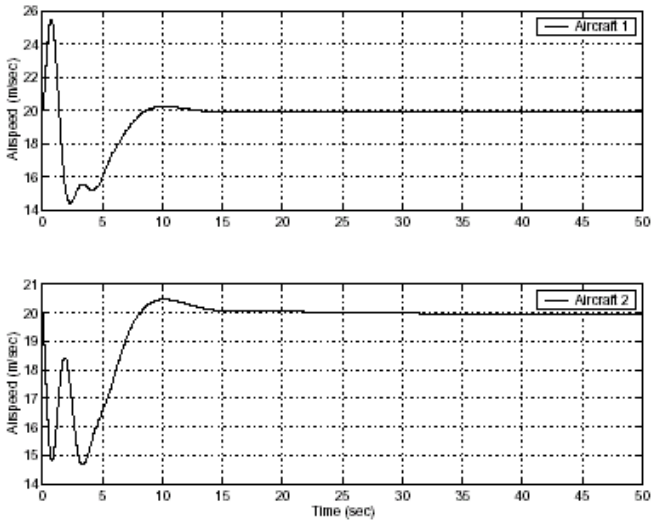

Figure 14. Airspeed time histories during formation geometry change.

The last simulation shows how the FC could reproduce the behavior of migrational birds. The initial condition is a steady-level flight. Each aircraft has an initial airspeed of 20 ft/sec that is the commanded trajectory. A speed perturbation is introduced on aircraft 2, which slows down with respect to aircraft 1. Figure 15 shows speed profiles for the two aircraft. It is clear how aircraft 1 stops following the prescribed velocity and 'waits' for aircraft 2 in order to maintain the nominal distances.

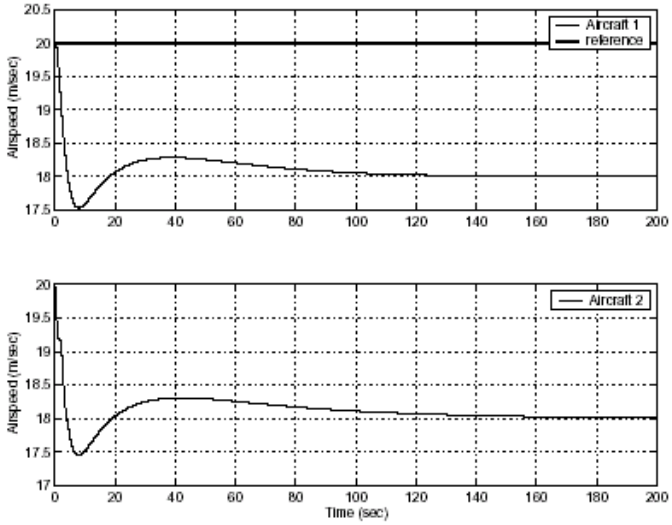

Figure 15. Airspeed time histories during perturbed flight.

Expert Guidance and Navigation Issues

In this section, a brief description of a waypoint apporach to guidance of unmanned air vehicles is presented. The work is relative to a single UAV, however current research is under way in order to extend the methodology to multiple cooperative aircraft.

A typical operation for an UAV in surveillance and search & rescue tasks can be with with a set of sequential waypoints to be passed by the aircraft. Since traditional proportional guidance techniques do not allow specifying desired waypoint's crossing direction, a fuzzy guidance scheme was developed. This allows a better trajectory description by specifying the single waypoint position in space, crossing heading and velocity. The procedure is based on a fuzzy controller that commands the aircraft, via its autopilot, to approach a list of waypoints. Implementation of a fuzzy guidance controller may be very expensive in terms of computational power/time, to solve this problem, a fuzzy controller was designed using a new approach based on Takagi-Sugeno fuzzy systems. This technique solves also previous 3 FGC version problems relative to non-smooth autopilot input generation.

The aircraft guidance problem is addressed, based on by an inner nonlinear control loop described previously in the paper, which allows tracking of commanded velocity , flight path, and heading angles. Then, an outer loop, that is the actual fuzzy guidance system (FGS), generates a reference path command in term of desired velocity, flight path and heading for the inner loop, in order to reach the desired waypoint. The Guidance System presented here is the evolution of the one presented by the authors in previous work. The main disadvantages of the old guidance system were the use of Mamdami Fuzzy networks that are too complex for real-time implementation, the use of triangular membership functions that resulted in too "square" trajectories and furthermore the fuzzy laws gave a good performance around the design aircraft speed only. One thing that remains unaltered from previous work is the use waypoint-relative coordinates to design guidance laws independently of waypoint orientation. To overcome the disadvantages of old approach, this new work proposes the use of Takagi-Sugeno Fuzzy networks with gaussian membership functions that helped generating smooth trajectories and resulted in less fuzzy sets and laws. Furthermore a non-linear scaling factor has been introduced to guarantee laws validity over a large speed range.

Two components constitute the guidance system: the Waypoint Generator (WG) and the Fuzzy Guidance System itself(FGS). The desired trajectory is specified in terms of a list of waypoints without any requirement on the path between two successive waypoints. A waypoint is given in cartesian-space coordinates (*Xw; Yw;Hw*), and a desired crossing speed (*Vw*) and heading angle (χw) are used to obtain a preferred approaching direction and velocity, thus the waypoint belongs a five-dimensional space $W = [Xw; Yw;Hw; Vw; \chi w]$. The WG holds a listof waypoints (WL) in 5-D, checks aircraft position, and updates the desired waypoint when the previous one has been reached within a given tolerance. When all waypoints have been reached, it holds the last one so that the aircraft loops around it. The waypoint generator's only task is to present the actual waypoint to the FGS. No dead-reckoning or navigational errors are modeled so the WG and the FGS know

the exact aircraft positions, velocity and heading. Between theWG and the FGS, a coordinate rotation system transforms earth-fixed-frame position errors into waypoint-frame relative errors. Each waypoint defines a coordinate frame centered in the waypoint position (*Xw; Yw;Hw*) and rotated by χw around the *H*-axis. This coordinate transformation allows the synthesis of a fuzzy rule-set valid in the waypoint-fixed coordinated frame that is invariant with respect to the desired approach direction . When a waypoint is reached, the next one is selected, the actual reference value W is changed and the rotation matrix is updated to transform position and orientation errors into the new waypoint coordinate frame.

As described above, the aircraft autopilots are designed to track desired airspeed, heading and flight path angles. Using the completed decoupled implementation of guidance laws, three independent Takagi-Sugeno Fuzzy Controller were designed to constitute the FGS.

One FC generates the desired flight path angle for the autopilot using altitude error

$$e_H = (H_w - H)$$

$$\gamma_d = f_\gamma(e_H)$$

The second fuzzy controller computes desired aircraft velocity:

$$V_d = V_w + f_V(V_w - V) = V_w + f_V(e_V)$$

The third, and most complex FC is demanded to generate the desired heading angle using the position errors along the *X* and *Y* axes of the actual waypoint-frame and heading error. A fuzzy rule-set designed at a fixed airspeed value can produce a lack of tracking performance when the desired waypoint crossing-speed *Vw* differs significantly from the design value. The solution to this problem is achieved by introducing a speed-depending scale coefficient for position errors leading to.

$$\chi_d = \chi_w + f_\chi(e^w_{X_C}, e^w_{Y_C}, e_\chi)$$

with

$$\begin{pmatrix} e^w_X \\ e^w_Y \end{pmatrix} = Rot(\chi_w) \cdot \begin{pmatrix} e_X \\ e_Y \end{pmatrix} = Rot(\chi_w) \cdot \begin{pmatrix} X_w - X \\ Y_w - Y \end{pmatrix}$$

$$\begin{pmatrix} e^w_{X_C} \\ e^w_{Y_C} \end{pmatrix} = S(V_w, V^*) \cdot \begin{pmatrix} e^w_X \\ e^w_Y \end{pmatrix}$$

$$S(V_w, V^*) = \frac{V^*}{V_w}$$

where *V** is the fuzzy design point airspeed. A schematic block diagram of the control structure is swhown in figure 16.

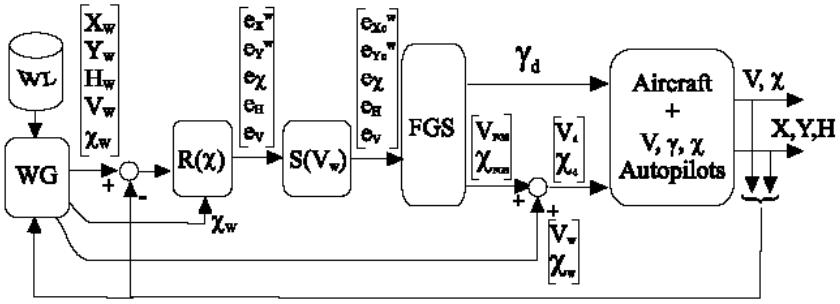

Figure 16. Implementation of Fuzzy guidance to a single UAV.

The fuzzy rules have been defined according to the desired approaching behavior and angular rates limitations of the aircraft. Fuzzy knowledge base was designed to generate flyable trajectories using the maximum linear and angular velocities and accelerations that are typical of a small propeller-engine aircraft.

The FGS provides with different desired flight path and heading angle commands for different values of distance from the waypoint. Based on the complete uncoupled aircraft model, it is possible to describe each fuzzy controller separately from the others. The Altitude and the Velocity FC systems are less complex than the Heading controller, and they are both implemented using Takagi-Sugeno model. For the first one the only input is the altitude error and four fuzzy set are designed to map this input and four for the desired output. The Velocity FC has similar complexity: 3 input fuzzy sets for the velocity error and 3 for the resulting desired output. As stated before, guidance in the horizontal (*X*-*Y*) plane is more complex than guidance in the vertical (*X* -*H*) plane. The horizontal plane fuzzy controller takes its inputs from scaled position errors and heading error. The scaled position error in the x-direction is coded into five gaussian fuzzy sets, while three sets are also defined for the scaled error in the y-direction. Considering the Takagi-Sugeno output function for this fuzzy controller:

$$y = \frac{\sum_{i=1}^{m} \mu_i(x) u_i}{\sum_{k=1}^{m} \mu_k(x)} = \frac{1}{c(x)} \sum_{i=1}^{S} \sum_{j=1}^{K} \mu_i^{xy}(e_{X_C}^w, e_{Y_C}^w) \cdot \mu_{ij}^{\chi}(e_\chi) u_{ij} = \frac{1}{c(x)} \sum_{i=1}^{S} \mu_i^{xy}(e_{X_C}^w, e_{Y_C}^w) \cdot \delta_{ij}^{\chi}(e_\chi)$$

S is the number of zone dividing the flight space and *K* is the number of subsets (dependent on the x-direction error) defined for each zone. The above equation can be simplified, yielding

$$\sum_{i=1}^{S} \frac{\mu_i^{xy}(e_{X_C}^w, e_{Y_C}^w)}{c(x)} \cdot \delta_{ij}^{\chi}(e_\chi) = \sum_{i=1}^{S} \overline{\mu}_i^{xy}(e_{X_C}^w, e_{Y_C}^w) \cdot \delta_{ij}^{\chi}(e_\chi)$$

Fixing the scaled errors in the middle of *P*th zone, under the assumption that the contribution from the other zones is near to zero:

$$y\Big|_{\substack{e_{X_C}^w \\ e_{Y_C}^w}} = \overline{\mu}_P^{xy}(e_{X_C}^w, e_{Y_C}^w) \cdot \delta_P^{\chi}(e_\chi) + \sum_{\substack{i=1 \\ i \neq P}}^{S} \overline{\mu}_i^{xy}(e_{X_C}^w, e_{Y_C}^w) \cdot \delta_{ij}^{\chi}(e_\chi) \cong \overline{\mu}_P^{xy}(e_{X_C^P}^w, e_{Y_C^P}^w) \cdot \delta_P^{\chi}(e_\chi)$$

The above equation shows that the definition of fuzzy sets for the x-direction error error should be computed looking at each single set partitioning the flight space, and then looking at cumulative result. Under this assumption seven fuzzy sets have been defined.

Figures 17 and 18 show the effect of parameter S previously defined; the trajectories maintain a smooth shape but the turn radius changes: in particular the turn radius increases at higher speed and decreases at speed lower than *V**.

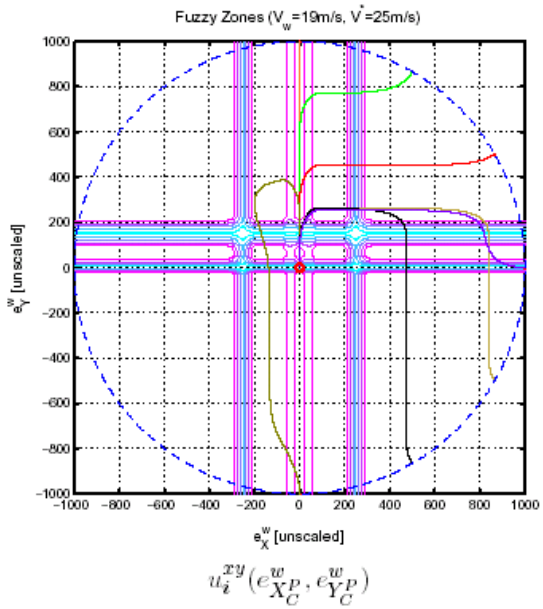

$u_i^{xy}(e_{X_C^P}^w, e_{Y_C^P}^w)$

Figure 17. Contour plots for membership functions

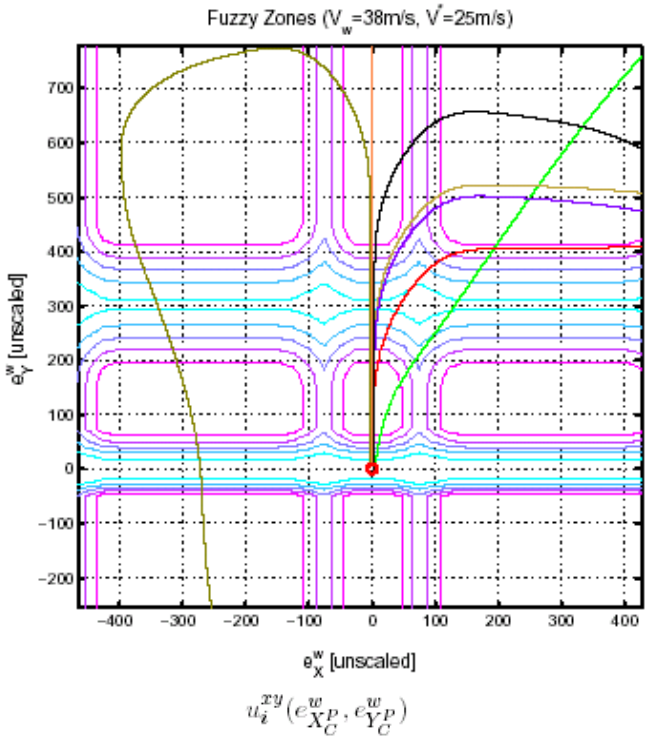

Figure 18. Contour plots for membership functions

Simulation Results

The following simulation shows the results of a non planar trajectory. First the aircraft is driven to waypoint *W*1, then to align with *W*2, then to *W*3 that is 150 meters lower in altitude and very near on the (*X,Y*) plane and finally to *W*4 that is at altitude 100 with a desired approach angle rotated by 90 degrees with respect to the previous waypoint. Figure 19 shows this trajectory. The required descent from W2 to W3 is too steep for the aircraft capabilities, as decided in the design phase of fuzzy rule-set. A s a matter of fact, when the aircraft reaches the *X,Y* coordinates of W3 its altitude is still too high, and it starts a turn to come back to the waypoint at the prescribed altitude. In fact, the aircraft begins a spiral or a 8-shaped descent, centered on the waypoint vertical axis, decreasing altitude with the descent rate limitation given by FGS, until the waypoint altitude is reached and then it proceeds to next waypoint. In this particular case, half turn is enough to reach W3 altitude, thus, when it reaches the desired altitude, it holds it and crosses successfully waypoint W3 and, successively, waypoint W4.

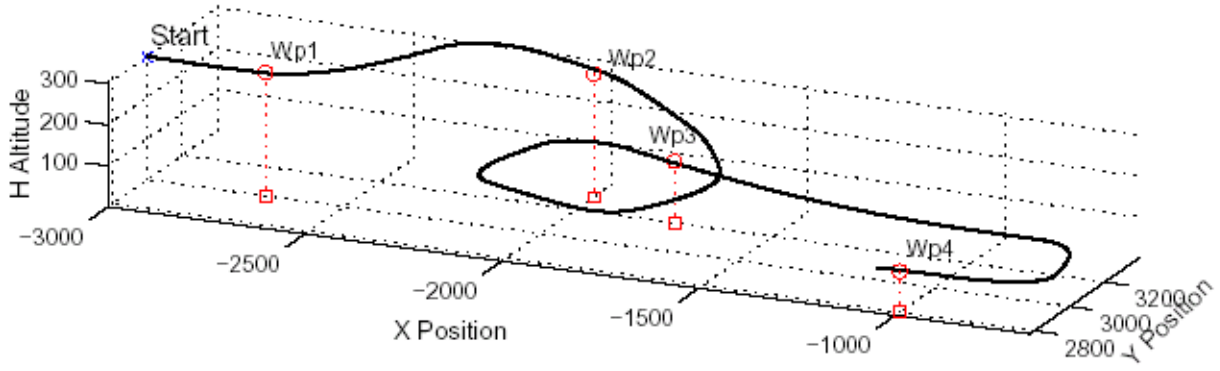

Figure 19. A 4-waypoint generated trajectory

Conclusions

The paper presents some issues on guidance, navigation and control problems related to unmanned aircraft. Methodolodgies based of maintaining desired formations shapes, and autonomous guidance were outlined.

References

[1] Bloy, A. W., West, M. G., Lea, K. A., and Jouma'a, M. "Lateral Aerodynamic Interference Between Tanker and Receiver in Air-to-Air Refuelling". *Journal of Aircraft*, Vol. 30 : pp. 705–710, 1993.
[2] Bloy, A. W. and Jouma'a, M. "Lateral and Directional Stability Control in Air-to-Air Refuelling". *ImechE, Part G Journal of Aerospace Engineering*, Vol. 209 : pp. 299–305, 1995.
[3] Myatt, J. H. and Blake, W. "Aerodynamics Database Issues for Modeling Close Formation Flight". In *Proceedings of AIAA Guidance, Navigation and Control Conference*, Portland, OR, August 1999.
[4] Gingras, D. "Experimental Investigation of a Multi-Aircraft Formation". In *Proceedings of AIAA Applied Aerodynamics Conference*, 1999.
[5] Gingras, D. and Player, J. "Static and Dynamic Wind Tunnel testing of Air Vehicles in Close Proximity". In *Proceedings of AIAA Atmospheric Flight Mechanics Conference*, Montreal, Quebec, Canada, August 2001.
[6] Nelson, R. C. and Jumper, E. J. "Aircraft Wake vortices and their Effect on Following Aircraft". In *Proceedings of AIAA Atmospheric Flight Mechanics Conference*, Montreal, Quebec, Canada, August 2001.
[7] Proud. A. W., Pachter, M., and D'Azzo, J. J. "Close Formation Flight Control". In *Proceedings of AIAA Guidance, Navigation and Control Conference*, Portland, OR, August 1999.
[8] Blake, W. and Multhopp, D. "Design, Performance and Modeling Considerations for Close Formation Flight". In *Proceedings of AIAA Guidance, Navigation and Control Conference*, Philadalphia, PA, August 1998.
[9] Houghton, E.L. and Brock, A.E. *"Aerodynamics for Engineering Students"*. Arnold Publishing, 1970.
[10] Buzogany, L. E., Pachter, M., and D'Azzo, J. J. "Automated Control of Aircraft in Formation Flight". In *Proceedings of AIAA Guidance, Navigation and Control Conference*, Monterey, CA, August 1993.
[11] Chichka, D. and Speyer, J. "Decentralized Controllers for Unmanned Aerial Vehicle Formation Flight". In *Proceedings of AIAA Guidance, Navigation and Control Conference*, San Diego, CA, July 1996.
[12] D. F. Chichka, J. L. Speyer, and C. G. Park. "Peak-Seeking Control with Application to Formation Flight". In *Proceedings of IEEE Conference on Decision and Control*, December 1999.
[13] J. J. D'Azzo M. Pachter and J.L. Dargan. "Automatic Formation Flight Control". *Journal of Guidance, Control and Dynamics*, 17(6):1380–1383, May 1994.
[14] M. Pachter, J. J. D'Azzo, and A. W. Proud. "Tight Formation Flight Control". *Journal of Guidance, Control and Dynamics*, 24(2):246–254, March-April 2001.
[15] C. Schumacher and R. Kumar. "Adaptive Control of UAVs in Close Formation Flight". In *Proceedings of American Control Conference*, Chicago, IL, June 2000.
[16] F. Giulietti, L. Pollini, and M. Innocenti. "Autonomous Formation Flight". *IEEE Control Systems Magazine*, 20(6):34–44, December 2000.
[17] Capetta, R., Giulietti, F., and Innocenti, M. "WakeCAD: Aerodynamic Interference Calculation Toolbox for Design, Simulation and Control of UAVs". In *Proceedings of AIAA Guidance, Navigation and Control Conference*, Montreal, Quebec, Canada, August 2001.
[18] Giulietti, F., Pollini, L., and Innocenti, M. "SNIPE: Development of an Unmanned Aerial Vehicle at DSEA". In *Proceedings of 15th Bristol International Conference on UAVs*, Bristol, UK, April 2000.
[19] M. R. Anderson and A. C. Robbins. "Formation Flight as a Cooperative Game". In *Proceedings of Aiaa Guidance, Navigation and Control Conference*, Philadelphia, PA, August 1998.
[20] J. Van Tyne and A.J. Berger. "*Fundamentals of Ornithology"*. John Wiley, 1976.
[21] M. Innocenti G.Mancino, M. Garofoli, and M. Napolitano. "Preliminary Analysis of Formation Flight Management". In *Proceedings of Aiaa Guidance, Navigation and Control Conference*, Portland, OR, August 1999.
[22] Takagi, T. and Sugeno, M., "Fuzzy Identification of systems and its applications to modeling and control," *IEEE Transaction on System Man and Cybernetics*, Vol. SMC, No. 15, Jan./Feb. 1985, pp. 116–132.
[23] Lin, C.-F., *Modern navigation, guidance and control processing*, Advanced Navigation Guidance and Control and their Applications, Prentice Hall, 1999.
[24] Giulietti, F., Pollini, L., and Innocenti, M., "Waypoint-based Fuzzy Guidance for Unmanned Aircraft," *Proceedings of* 15*th IFAC Symposium on Automatic Control in Aerospace, Bologna, IT.*, 2001.

[25] Pollini, L., Giulietti, F., and Innocenti, M., “SNIPE: Development of an Unmanned Aerial Vehicle at DSEA - University of Pisa,” *Proceedings of 15th Bristol International Conference on UAVs Conference 2000, Bristol, UK.*, 2000.
[26] Pollini, L., Giulietti, F., and Innocenti, M., “SNIPE: Development of an Unmanned Aerial Vehicle at DSEA - University of Pisa,” *Proceedings of UAV 2000 Conference, Paris, FR.*, 2000.